

AEROELASTIC OPTIMISATION OF A CANTILEVERED PLATE WITH LOCAL DAMPING APPLICATION

Ali Tatar^{1,2}, Stephane Fournier², Jonathan E. Cooper²

¹ Istanbul Technical University, Faculty of Aeronautics and Astronautics
Ayazaga Campus, 34469, Maslak/Istanbul, Turkey
tataral@itu.edu.tr

² University of Bristol, Department of Aerospace Engineering
Queen's Building, University Walk, Bristol, BS8 1TR, UK
ali.tatar@bristol.ac.uk, stephane.fournier@bristol.ac.uk, j.e.cooper@bristol.ac.uk

Keywords: aeroelasticity, flutter, damping, optimisation, fixed wing

Abstract: This paper aims to optimise the aeroelastic performance of a cantilevered plate through the application of a local damping distribution. An aeroelastic model was built in MSC Nastran 2018 using the finite element method and double lattice method for the structural and aerodynamic modelling of the cantilevered plate, respectively. For the aeroelastic flutter analyses, the number of structural and aero elements was determined based on the convergence study results. Stiffness proportional damping was employed to numerically model local damping as viscous, which allows both time and frequency domain simulations. Initially, case study analyses for structural and aeroelastic responses on the cantilevered plate model were conducted to find the sensitive local damping locations. It has been shown that maximum modal damping can be achieved by applying local damping at the maximum strain energy regions. Then, a genetic algorithm optimisation was employed to determine the optimised local damping application region for maximizing the flutter speed. It has been found that flutter speeds can be significantly shifted with the addition of local damping and higher modal damping can be achieved at maximum modal strain energy regions in aeroelastic flutter modes. This study highlights the potential usage of local damping in the structural design of wings and suggests a pathway toward practical passive local damping distribution.

1 INTRODUCTION

Lighter aircraft wing structures would decrease fuel consumption and improve the environmental performance in the aerospace industry, where composite materials are commonly used, due to their higher specific strength. On the other hand, a weight reduction can increase the flexibility of the aircraft wing structure, which can lead to unwanted aeroelastic stability problems, e.g. divergence and flutter, and higher aeroelastic-induced vibrations [1].

Conventionally, modification of the aeroelastic behaviour, known as aeroelastic tailoring, is carried out at the aircraft wing design stages to improve aircraft performance under various flight conditions [2–5]. For this purpose, the stiffness and mass parameters of wing skins are passively tuned along the wing. Moreover, additional structural damping is required to overcome undesirable aeroelastic stability and vibration issues [6]. It is well known that structural damping has a

stabilizing effect on aircraft wings [7]. However, less research has been carried out to investigate the effect of local damping on the aeroelastic performance of aircraft wings [8], [9] and these studies have focused on the identification of structures containing non-proportional damping.



Figure 1: Airbus eXtra Performance Wing demonstrator.

Since the go-to material employed in aircraft structures has and will be increasingly shifting toward composite materials. Composite materials already present a higher level of damping compared to aerospace grade metallic alloys, moreover, due to their nature, they can also be produced using several types of constituents and additives to increase their ability to absorb deformation energy [10–13].

Aeroelastic optimization with local damping application involves a combination of advanced materials, innovative design techniques, and comprehensive computational models [14]. The integration of both active and passive damping methods, along with sophisticated optimization algorithms, significantly enhances the aeroelastic performance of aircraft wings. Continued research in this domain is crucial for further improvements in the efficiency, safety, and overall performance of modern aircraft [15]. Local damping techniques play a crucial role in mitigating aeroelastic instabilities such as flutter, leading to improved safety and efficiency of the aircraft.

The main aim of this paper is to investigate the feasibility of the use of added targeting local damping on a cantilevered plate, representing an aircraft wing, in order to passively increase the modal damping and flutter speeds. Determining the optimum local damping distribution along the cantilevered plate for improving aeroelastic performance is the main objective of this paper. For this purpose, an aeroelastic model is built with the finite element method and double lattice method in MSC Nastran 2018 for the structural and aerodynamic modelling of the cantilevered plate, respectively. The number of structural and aero elements is determined from the modal and aeroelastic convergence study results. Stiffness proportional damping ($D = \beta * E$) is used for numerical modelling of both global and local damping on the cantilevered plate. Local damping case studies and genetic algorithm optimisation are employed to determine the best local damping application regions along the cantilevered plate for maximising the flutter speed and modal damping. A genetic algorithm-based in-house optimisation code is created by combining MATLAB 2021a and MSC Nastran 2018.

2 CANTILEVERED PLATE MODEL DESCRIPTION

2.1 Structural Model

A cantilevered plate finite element (FE) model was generated with two-dimensional CQUAD4 shell elements in MSC Nastran 2018, as shown in Figure 2. In total, 128 CQUAD4 elements were employed for generating the global finite element model. The number of elements was determined with the natural frequency convergence study. This model was used for the structural and aeroelastic optimisation studies. It should be noted that all translational and rotational degrees of freedom were locked at the root of the cantilevered plate.

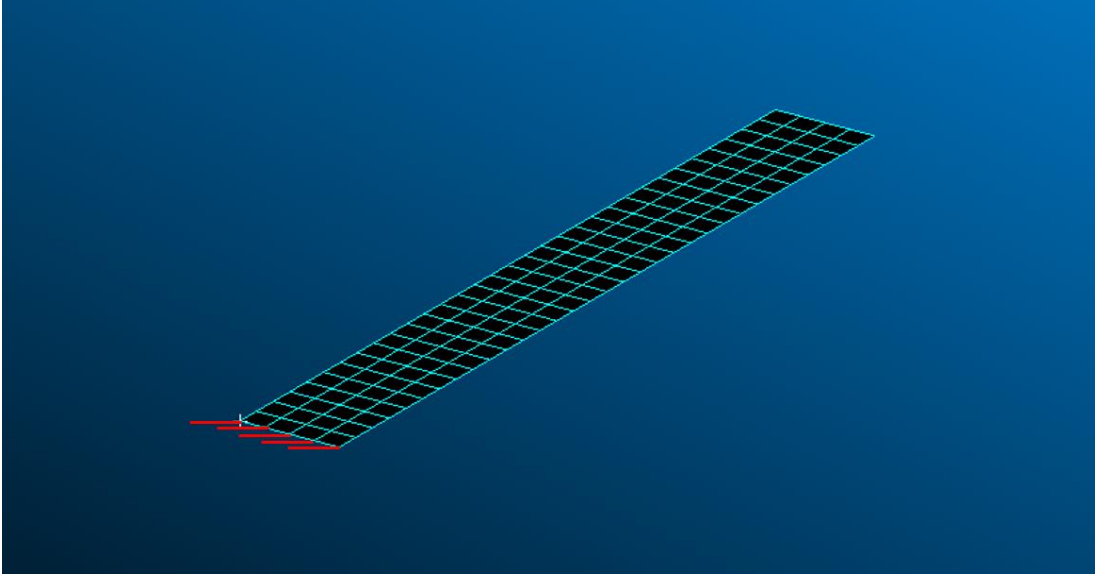


Figure 2: Structural FE model of the cantilevered plate.

This cantilevered plate is made of Aluminium material. It has a 4-meter span and 0.5-meter chord lengths with 0.03-meter thickness and its material properties are presented in Table 1.

Table 1: Aluminium material properties.

Property	Value
Elastic Modulus [GPa]	70
Poisson`s Ratio	0.3
Density [kg/m ³]	2700

2.2 Damping Model

Rayleigh damping model, also known as proportional damping, was used in this study. Rayleigh damping formula is given as

$$\mathbf{D} = \alpha\mathbf{A} + \beta\mathbf{E} \quad (1)$$

where \mathbf{A} and \mathbf{E} are structural mass and stiffness matrices, respectively. α and β are the Rayleigh damping coefficients which is a linear combination of the structural mass and stiffness matrices.

The Rayleigh damping coefficients α and β can be defined as

$$\alpha = \frac{2\omega_a\omega_b(\zeta_b\omega_a - \zeta_a\omega_b)}{\omega_a^2 - \omega_b^2}$$

$$\beta = \frac{2(\zeta_a\omega_a - \zeta_b\omega_b)}{\omega_a^2 - \omega_b^2}$$
(2)

where ω_a and ω_b are the bounding frequencies. ζ_a and ζ_b are the damping ratios at these frequencies [16].

Table 2: Damping parameters.

Property	Value
Bounding Frequency ω_a [Hz]	0
Bounding Frequency ω_b [Hz]	30
Lower Global Damping Ratio	0.5 %
Higher Global Damping Ratio	10.5 %
Local Damping Ratio	10 %

The damping parameters used in this study are summarised in Table 2 below. It is important to point out that setting the bounding frequency ω_a as 0 Hz makes Rayleigh damping coefficients α zero. Hence, Equation 1 converts into stiffness proportional form as

$$\mathbf{D} = \beta\mathbf{E}$$
(3)

Stiffness proportional form can give more robust results when using local damping application. In the local damping case studies and genetic algorithm optimisation study in Sections 4 and 5, 12.5 percent of the structure will be used for the local damping application, which makes the number of locally damped elements sixteen.

2.3 Aeroelastic Model

The doublet-lattice method is a commonly used method for aerodynamic analysis in subsonic conditions. Since our flight envelope is in subsonic condition, an aerodynamic model of the cantilevered plate was created using the Doublet-Lattice method in MSC Nastran 2018.

The general form of the full aeroelastic equations is written as

$$\mathbf{A}\ddot{\mathbf{q}}(t) + (\rho V\mathbf{B} + \mathbf{D})\dot{\mathbf{q}}(t) + (\rho V^2\mathbf{C} + \mathbf{E})\mathbf{q}(t) = 0$$
(4)

Here, \mathbf{A} , \mathbf{B} , \mathbf{C} , \mathbf{D} and \mathbf{E} are the structural mass, aerodynamic damping, aerodynamic stiffness, structural damping and structural stiffness matrices, respectively. ρ and V are the air density and free stream velocity. $\mathbf{q}(t)$ also represents the generalized coordinate.

The number of aerodynamic meshes was determined as 512 after the aeroelastic flutter convergence study. To couple aerodynamic and structural models, finite plate spline was used in MSC Nastran 2018.

3 DESIGN SPACE EXPLORATION

Exploring the design space of wings is a crucial activity in order to have an initial idea about their structural and aeroelastic responses. In this section, the design space of the cantilevered plate model will be explored with the modal and aeroelastic analyses.

3.1 Modal Analysis

Modal analysis is an essential tool for understanding the dynamic behaviour of the structure and model reliability. Therefore, a modal analysis was done in MSC Nastran 2018 using the normal mode analysis solver (SOL103) for the cantilevered plate model. The first six vibration modes of the wing are shown and summarised in Figure 3 and Table 3, respectively.

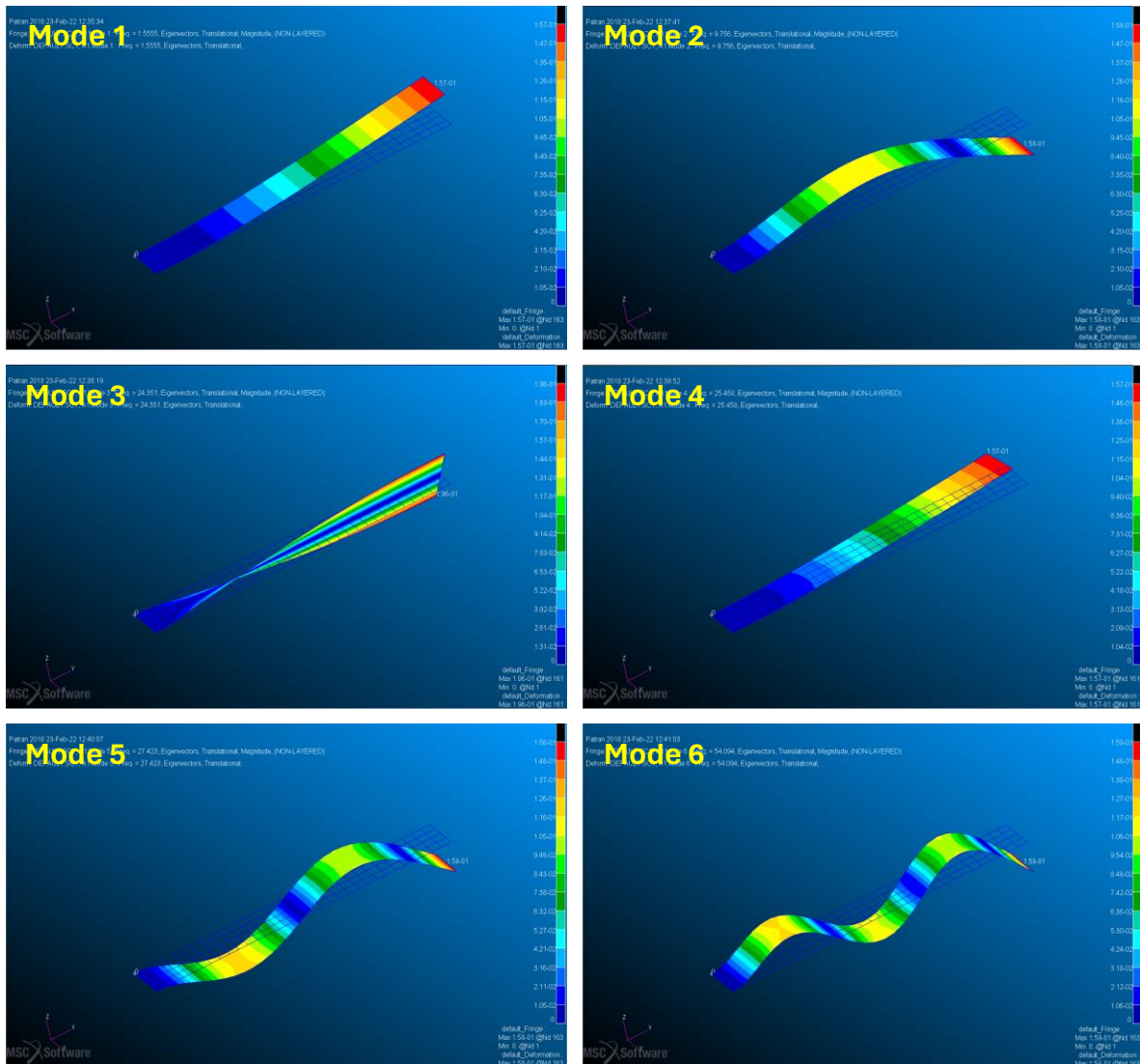


Figure 3: Modal analysis of the cantilevered plate.

It has been found that the first six vibration modes are global modes. No local modes are also detected at lower modes. Briefly, the modes are identified as out of plane bending, in-plane bending and torsional.

Table 3: Vibration modes.

Mode #	Mode Type	Natural Frequency [Hz]
1	Out of Plane Bending	1.6
2	Out of Plane Bending	9.8
3	Torsional	24.4
4	In Plane Bending	25.5
5	Out of Plane Bending	27.4
6	Out of Plane Bending	54.1

3.2 Aeroelastic Flutter Analysis

Aeroelastic flutter analyses were initially performed on the cantilevered plate model in MSC Nastran 2018 using the aeroelastic flutter analysis solver (SOL145) for the cases (i) no structural damping, (ii) lower global structural damping (0.5%) and (iii) higher global structural damping (10.5%). As provided in Table 2, bounding frequencies ω_a and ω_b were selected as 0 Hz and 30 Hz, respectively, for all structural damped cases.

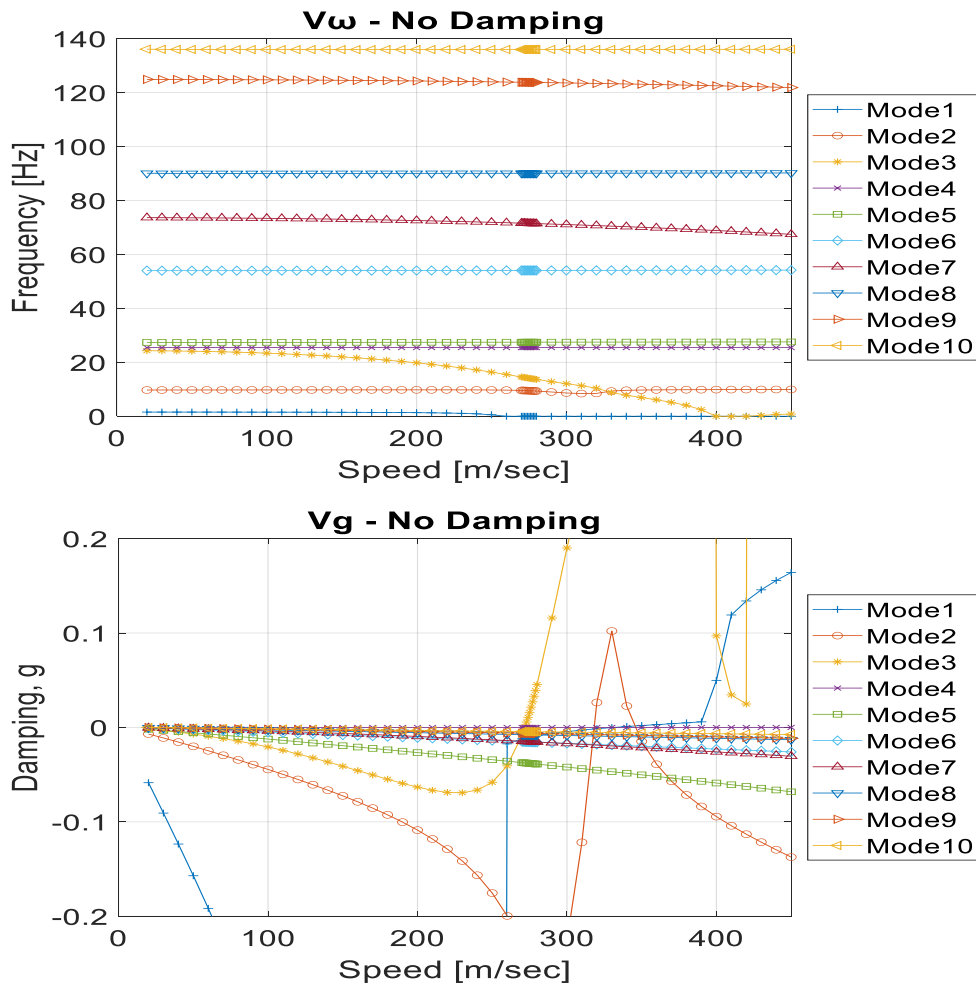


Figure 4: Frequency and damping versus speed maps for the no structural damping case.

Speed versus damping and speed versus natural frequency plots for the no structural damping case are shown in Figure 4. It is clearly seen that the flutter mechanism is between the 2nd and 3rd modes which are out of plane and torsional modes. These modes are becoming coupled at the flutter speed, which is 271.8 m/sec. The aeroelastic flutter mode shape at 271.8 m/sec is seen in Figure 5. Its frequency was detected at 14.4 Hz. In this figure, coupled bending and torsional mode is clearly seen, which confirms the aeroelastic flutter coupling mechanism between the out of plane bending and torsional modes.

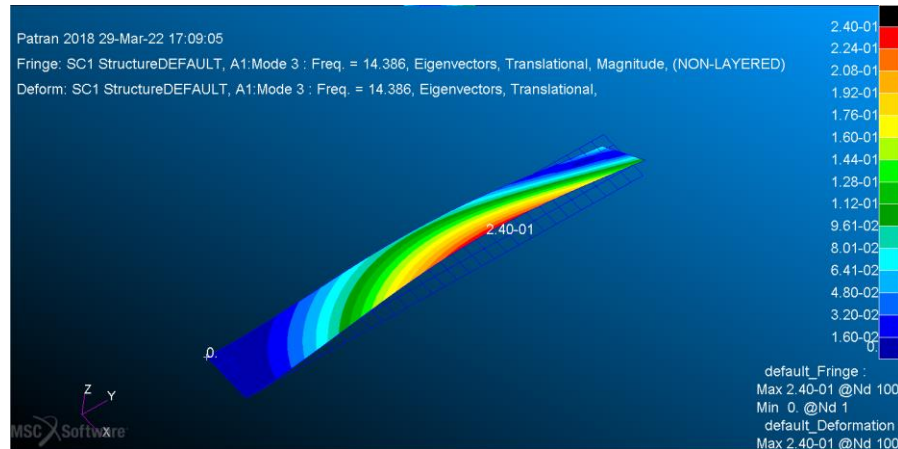


Figure 5: Aeroelastic flutter mode shape for the no structural damping case.

Furthermore, flutter speeds for the lower global damping (0.5%) and higher global damping (10.5%) were found to be at 274.5 m/sec and 303.8 m/sec, respectively. It has been observed that flutter speed can be shifted with the addition of structural damping. The flutter speed results of all cases are compared in Section 5.2.

4 LOCAL DAMPING CASE STUDY ANALYSES

In engineering, case study analysis is a commonly used technique to understand how the system parameter can significantly affect the output response of a system. It can be a helpful tool to identify which system parameters most affect the performance of a system before starting the actual optimisation studies. In this section, structural and aeroelastic case study analyses were conducted with sixteen locally damped elements, which cover 12.5 percent of the structure.

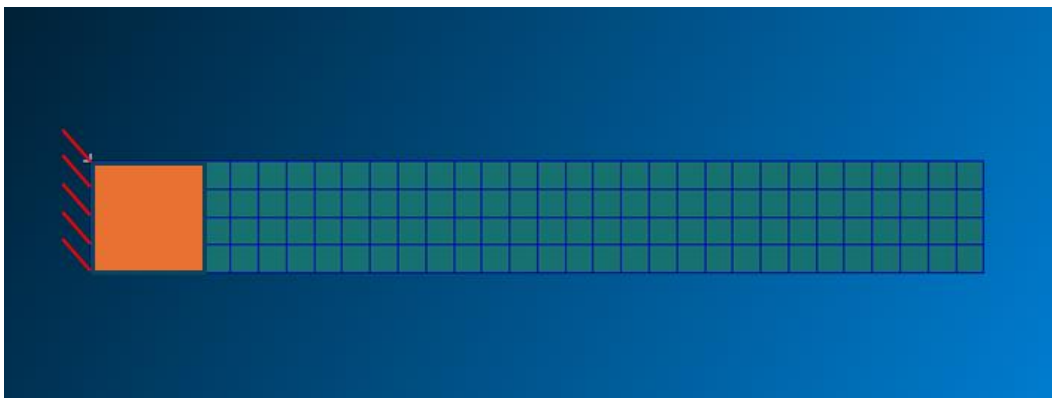


Figure 6: Local damping elements on the cantilevered plate.

In order to find the most sensitive damping region in terms of modal damping and aeroelastic flutter speed values, sixteen locally damped elements (4 x 4 block) on the cantilevered plate model were shifted thirty-two times from root to tip in the spanwise direction, as seen in Figure 6. It should be noted this cantilevered plate consists of 32 (span) x 4 (chord) meshes.

Stiffness proportional damping ($D = \beta * E$) was employed and Rayleigh damping coefficient β was calculated using the Equation 2, as explained in Section 2.2. It should be noted the damping ratio parameters given in Table 2 were employed in this equation. 0.5 percent lower global damping (ζ) was applied on the whole structure and 10 percent local damping (ζ) was employed in the structural and aeroelastic case study analyses.

4.1 Modal Damping

Natural frequency and modal damping sensitivity to the location of damping elements were plotted for the first eight modes as shown in Figure 7.

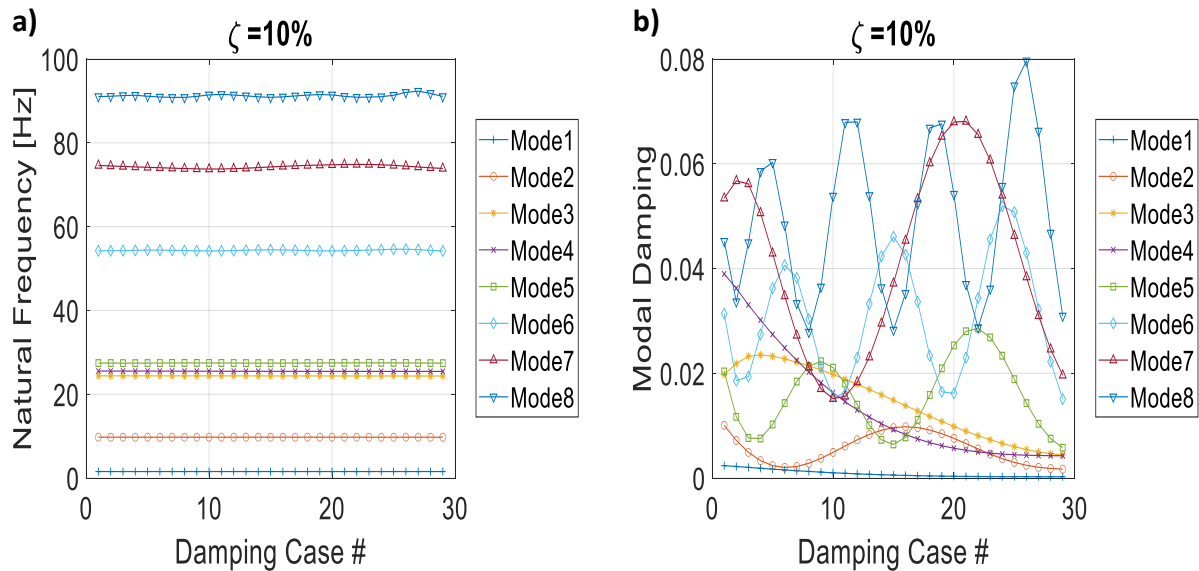


Figure 7: Sensitivity of modal parameters to the location of damping elements from root to tip, a) natural frequency, b) modal damping.

It has been found that the highest modal damping can be achieved at the mode shape curvatures and root of the cantilevered plate. It should be noted that the highest modal strain energy also occurs at the mode shape curvature and root, highlighting the relationship between the modal strain energy and local damping application region. Practically, local damping should be applied at the highest modal strain energy regions in order to achieve the highest modal damping benefit.

4.2 Aeroelastic Flutter Speed

To investigate the flutter speed sensitivity to the structural damping, the position of the local damping elements was shifted from the root to the tip of the cantilevered plate. Flutter speeds change between 284 m/sec and 274.5 m/sec with the addition of local damping elements. Maximum flutter speed is found to be at 283.9 m/sec, which is closer to the root (not exactly at the root) as seen in Figure 8. It is important to point out that the maximum flutter speed location has nearly the highest modal strain energy at the aeroelastic flutter mode shape, which is consistent with the modal damping results in section 4.1.

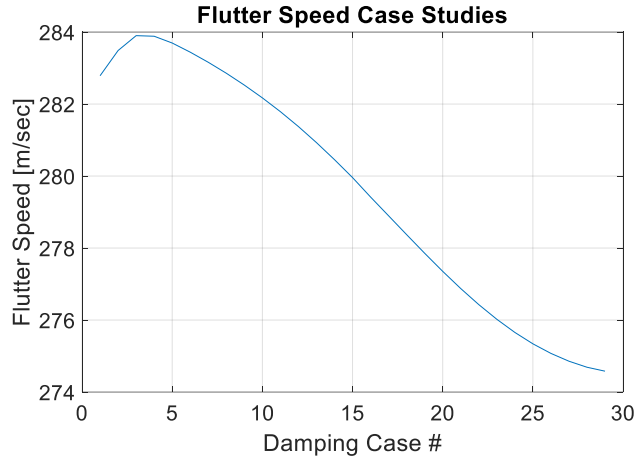


Figure 8: Sensitivity of flutter speed to the location of damping elements from root to tip.

5 AEROELASTIC OPTIMISATION

In the field of aeroelasticity, genetic algorithms, particle swarm, gradient-based, surrogate-based and machine learning-based optimisation are commonly used optimisation methods [1,3,4]. In this study, a genetic algorithm (GA) has been selected and an in-house optimisation code called NPDAMP has been developed using MATLAB 2021a coupled with the MSC Nastran 2018 aeroelastic flutter (SOL145) solver at the University of Bristol.

In the aeroelastic optimisation, the design objective is set as maximising the flutter speed; thus, it is a “single objective” optimisation problem. The design variables are the locations of the sixteen damping elements. These sixteen damping elements are independent design variables. It should be noted that they are not dependent on each other and not moving together. The design response is only the aeroelastic flutter analysis. The design constraint is the total number of damping elements.

5.1 Flutter Speed Optimisation

In the flutter speed optimisation, the genetic algorithm searched the best local damping application region on the cantilevered plate so as to maximise the flutter speed. Optimised flutter speed was found to be at 284.6 m/sec after the three hundred iterations. It should be noted that 0.5 percent lower global damping, applied on the whole structure, and 10 percent local damping were employed in the aeroelastic flutter speed optimisation.

1	5	9	13	17	21	25	29	33	37	41	45	49	53	57	61	65	69	73	77	81	85	89	93	97	101	105	109	113	117	121	125
2	6	10	14	18	22	26	30	34	38	42	46	50	54	58	62	66	70	74	78	82	86	90	94	98	102	106	110	114	118	122	126
3	7	11	15	19	23	27	31	35	39	43	47	51	55	59	63	67	71	75	79	83	87	91	95	99	103	107	111	115	119	123	127
4	8	12	16	20	24	28	32	36	40	44	48	52	56	60	64	68	72	76	80	84	88	92	96	100	104	108	112	116	120	124	128

Figure 9: GA optimised local damping region for maximising the flutter speed.

The genetic algorithm optimised local damping region with the sixteen damping elements is shown in Figure 9, which has the highest modal strain energy along the structure. When comparing with the aeroelastic case study analyses, the optimised local damping region for maximising the flutter speed gives the higher modal strain energy at the aeroelastic flutter mode shape.

5.2 Comparison of Results

The flutter speed results of the selected configurations which are undamped (baseline), lower global damping (0.5%), higher global damping (10.5%), best case study (global (0.5%)+local (10%)) and GA optimisation (Global (0.5%)+Local (10%)) are presented in Table 4. Speed versus damping plots for these configurations are also shown in Figure 10.

Table 4: Flutter speeds of all cases.

Configurations	Configuration #	Flutter Speed [m/sec]	Change %
Undamped (Baseline)	C-1	271.80	0.00
Lower Global Damping (0.5%)	C-2	274.48	0.98
Higher Global Damping (10.5%)	C-3	303.80	11.77
Best Case Study (Global (0.5%)+Local (10%))	C-4	283.90	4.45
GA Optimisation (Global (0.5%)+Local (10%))	C-5	284.63	4.72

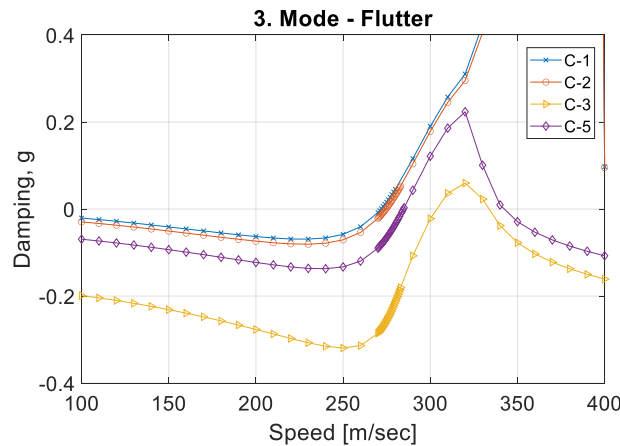


Figure 10: Comparison of speed versus damping plots of all cases.

It is found that the case study analyses and GA optimisation achieved 4.45% and 4.72% flutter speed increase with respect to the undamped (baseline) configuration. This achievement highlights the importance of local damping applications for maximising the flutter speed. Modal strain energy distribution of undamped and GA optimised local damped cases are also shown in Figure 11. It is seen that modal strain energy distribution slightly changes due to the local damping effect.

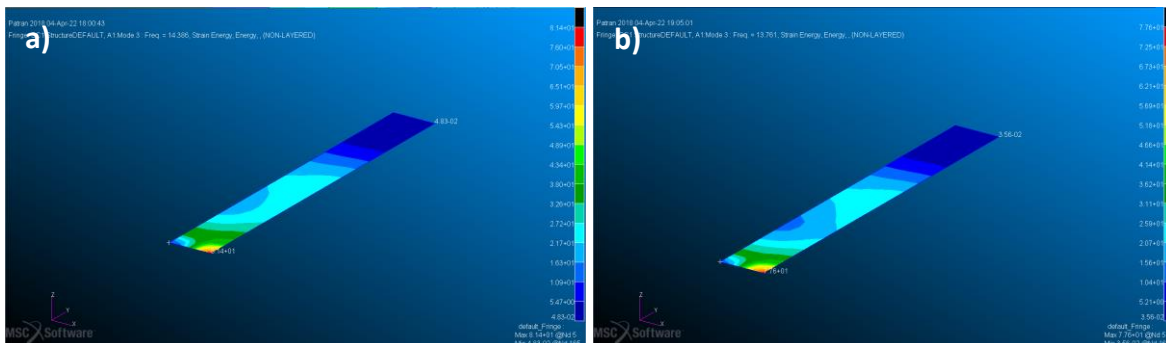


Figure 11: Flutter modal strain energy, a) undamped (C-1), b) GA optimised damped (C-5).

6 CONCLUSIONS

The possibility of maximising the flutter speed of a cantilevered plate with local damping application has been investigated in this study. Best local damping application regions along the cantilevered plate for maximising the flutter speed were found with the modal and aeroelastic case study analyses and genetic algorithm optimisation. Initially, modal and aeroelastic analyses were conducted to investigate the structural and aeroelastic responses and to determine the initial design space boundaries. A genetic algorithm-based optimisation methodology was developed and implemented using MATLAB 2021a and MSC Nastran 2018 for creating an in-house optimisation code.

Flutter speeds can be significantly maximised with the addition of local damping. It has been found that the flutter speed could increase by 4.45% and 4.72% compared to the undamped (baseline) configuration with case study analyses and GA optimisation, respectively. Higher modal damping has also been found to be at local damping application at maximum modal strain energy regions in the aeroelastic flutter modes. In practice, the authors suggest applying local damping at the highest modal strain energy regions for obtaining the highest modal damping and maximising flutter speed.

This research study highlights the potential usage of local damping applications for maximising the flutter speed in the structural design of wings. It also provides practical guidance for the local damping distribution. Further investigation on novel material damping schemes, particularly for composite structures is required in order to apply local damping to a structure more realistically.

ACKNOWLEDGEMENT

The authors acknowledge funding from the DAWS (Development of Advanced Wing Solutions) project supported by the ATI Programme, a joint Government and industry investment to maintain and grow the UK's competitive position in civil aerospace design and manufacture. The programme, delivered through a partnership between the Aerospace Technology Institute (ATI), Department for Business, Energy and Industrial Strategy (BEIS) and Innovate UK, addresses technology, capability and supply chain challenges. The first author was also supported by Research Fund of the Istanbul Technical University under Project Number: 45809.

REFERENCES

- [1] O. Stodieck, Aeroelastic Tailoring of Tow-Steered Composite Wings, Ph.D. Thesis, University of Bristol, 2016. <https://doi.org/10.13140/RG.2.2.29020.82562>.
- [2] O. Stodieck, J.E. Cooper, P.M. Weaver, P. Kealy, Improved aeroelastic tailoring using tow-steered composites, *Compos. Struct.* 106 (2013) 703–715. <https://doi.org/10.1016/j.compstruct.2013.07.023>.
- [3] O. Stodieck, J.E. Cooper, P.M. Weaver, P. Kealy, Optimization of tow-steered composite wing laminates for aeroelastic tailoring, *AIAA J.* 53 (2015) 2203–2215. <https://doi.org/10.2514/1.J053599>.
- [4] O. Stodieck, J.E. Cooper, P.M. Weaver, P. Kealy, Aeroelastic tailoring of a representative wing box using tow-steered composites, *AIAA J.* 55 (2017) 1425–1439. <https://doi.org/10.2514/1.J055364>.

- [5] O. Stodieck, G. Francois, D. Heathcote, E. Zypeloudis, B.C. Kim, A.T. Rhead, D. Cleaver, J.E. Cooper, Experimental validation of tow-steered composite wings for aeroelastic design, 17th Int. Forum Aeroelasticity Struct. Dyn. IFASD 2017. 2017–June (2017) 1–16.
- [6] S. Adhikari, Damping models for structural vibration, Ph.D. Thesis, University of Cambridge, 2001.
- [7] F. Beheshtinia, R.D.D. Firouz-Abadi, M. Rahmanian, Viscous damping effect on the aeroelastic stability of subsonic wings: Introduction of the U–K method, *J. Fluids Struct.* 73 (2017) 1–15. <https://doi.org/10.1016/j.jfluidstructs.2017.05.006>.
- [8] M. Eugeni, F. Saltari, F. Mastroddi, Structural damping models for passive aeroelastic control, *Aerosp. Sci. Technol.* 118 (2021) 107011. <https://doi.org/10.1016/j.ast.2021.107011>.
- [9] S. Naylor, M.F. Platten, J.R. Wright, J.E. Cooper, Identification of Multi-Degree of Freedom Systems With Nonproportional Damping Using the Resonant Decay Method, *J. Vib. Acoust.* 126 (2004) 298–306. <https://doi.org/10.1115/1.1687395>.
- [10] A. Treviso, B. Van Genechten, D. Mundo, M. Tournour, Damping in composite materials: Properties and models, *Compos. Part B Eng.* 78 (2015) 144–152. <https://doi.org/10.1016/j.compositesb.2015.03.081>.
- [11] F.-S. Liao, A.-C. Su, T.-C.J. Hsu, Vibration Damping of Interleaved Carbon Fiber-Epoxy Composite Beams, *J. Compos. Mater.* 28 (1994) 1840–1854. <https://doi.org/10.1177/002199839402801806>.
- [12] H.A. Scarton, I. Kahn, M.A. Rafiee, J. Rafiee, K. Wilt, N. Koratkar, Evidence of Coulomb Friction Damping in Graphene Nanocomposites, in: Vol. 13 Sound, Vib. Des., ASMEDE, 2010: pp. 183–187. <https://doi.org/10.1115/IMECE2010-39378>.
- [13] N.C. Adak, K.J. Uke, T. Kuila, Experimental and Finite Element Analysis of Free Vibration Behaviour of Graphene Oxide Incorporated Carbon Fiber/Epoxy Composite, *Compos. Res.* 31 (2018) 311–316. <https://doi.org/https://doi.org/10.7234/composres.2018.31.6.311>.
- [14] J. Najmi, H.A. Khan, S.S. Javaid, A. Hameed, F. Siddiqui, Aeroelastic tailoring for aerospace applications, *Heliyon.* (2024).
- [15] A. Tatar, R.C.M. Cheung, J.E. Cooper, D.P. Pearson, C. Warsop, Aeroelastic tailoring optimisation of a combat aircraft wing with tow-steered composites, in: 19th Int. Forum Aeroelasticity Struct. Dyn. IFASD 2022, 2022.
- [16] J.R. Wright, J.E. Cooper, Introduction to Aircraft Aeroelasticity and Loads, 2nd ed., John Wiley & Sons, 2015. <https://doi.org/10.1002/9781118700440>.

COPYRIGHT STATEMENT

The authors confirm that they, and/or their company or organisation, hold copyright on all of the original material included in this paper. The authors also confirm that they have obtained permission from the copyright holder of any third-party material included in this paper to publish it as part of their paper. The authors confirm that they give permission or have obtained permission from the copyright holder of this paper, for the publication and public distribution of this paper as part of the IFASD 2024 proceedings or as individual off-prints from the proceedings.